Optica Applicata, Vol. XLII, No. 1, 2012
DOI: 10.5277/oa120103

An on-line phase measuring profilometry based on modulation

WU YINGCHUN, CAO YIPING*, LU MINGTENG, LI KUN

Department of Opto-electronics Science and Technology, Sichuan University, Chengdu, P.R. China

*Corresponding author: ypcao@scu.edu.cn

An on-line phase measuring profilometry (PMP) based on Stoilov's algorithm which can be used for on-line 3-D shape inspection is proposed in this paper. A stationary sinusoidal grayscale fringe pattern is projected onto the object kept on the production line, and an immobile charge-coupled device (CCD) is used to capture five deformed patterns equidistantly. The phase distribution is calculated by using Stoilov's algorithm, and the height distribution of the inspected object is obtained through the relation of phase–height mapping. When inspected object moves, the positions of images in different deformed patterns change, so the pixel matching is implemented to acquire the equivalent phase-shifting which meets the requirement of Stoilov's algorithm. Modulation which represents the contour of inspected object is used as the template to perform the pixel matching for the first time in this paper. Computer simulation and experiment verified the effectiveness of the method.

Keywords: on-line inspection, phase measuring profilometry (PMP), Stoilov's algorithm, pixel matching, modulation.

1. Introduction

Due to the advantages of non-contacting operation, higher speed, accuracy, and easier implementation, optical 3-D shape measurement for deformable and motional object has a huge potential for applications in many areas, including industrial manufacturing, on-line inspection, reverse engineering, computer graphics, plastic surgery, security checks, *etc*. With the advanced development of optics, optoelectronics and the computer technique, the possibility has increased greatly for 3-D shape measurement to be achieved at a higher speed, higher degree of accuracy, and more handy [1].

A variety of optical 3-D shape measurement methods have been proposed to deal with dynamic and motional objects [2–8]. As a simple method in fringe projection profilometry, Fourier transform profilometry (FTP) has been extensively studied in recent years [2, 3]. XIANYU SU *et al*. discussed a 3-D shape measurement method of dynamical object based on FTP and successfully measured a man's chest of low breathing [4]. He quoted FTP in hydromechanical measurement field to measure and display the process of eddy generation and deepening [5]. The above methods are based on Fourier spectrum analyzing, which only needs one captured image, so the measure-

ment speed is fast, but at the cost of reducing the accuracy. Using color to code the patters, LI ZHANG *et al*. developed a color structured light technique for high-speed scans of moving objects [6]. SONG ZHANG *et al*. proposed a real-time 3-D shape measurement system [7, 8], which can be used for the measurement of dynamical objects. He had successfully measured the facial expression changes of a smiling person.

As a common method in three-dimensional sensing, phase measuring profilometry (PMP) has a huge potential in on-line inspection for its low cost and high accuracy. In this method, a stationary sinusoidal grayscale fringe pattern is projected onto the measured object, and a charge-coupled device (CCD) is used to capture a sequence of deformed patterns. If the object before the CCD is moving, the positions of object's image in different patterns obviously change. If the phase-shifting can be produced by the post-processing of the deformed patterns according to the change of the positions of object's image, the digital phase-shifting can be replaced and the phase of object can be calculated. However, the post-processing such as images' pixel matching of the deformed patterns is difficult, because the contour of the object is covered by the stripes. If we extract the object's contour from the deformed patterns by means of some digital image processing technology and use the contour to implement pixel matching, this will extend the application scope of the traditional PMP to inspect the moving objects.

The modulation of the object can well reflect the contour of the measured object [9]. So a novel on-line 3-D shape inspection method for obtaining equivalent phase-shifting step using modulation is discussed in this paper. And a reasonable choice of improved Stoilov's algorithm successfully lessens the requirement for accuracy of phase-shifting step, which makes the PMP more suitable for on-line inspection in automatic assembly line.

2. Principle

In on-line inspection, the measured object moves with uniform speed. If we can obtain the phase shifting by means of movement of the object instead of digital phase-shifting, the phase distribution of deformed pattern can be calculated by phase-shifting algorithm [10–12]. Figure 1 shows the layout of the inspected system; a computer graphics card sends a stationary sinusoidal grayscale fringe image signal to a digital light processing (DLP) projector that projects image onto the moving object [13]. A CCD is used to capture N frames deformed patterns with a constant frame rate when the object is moving. The captured images are then digitized by a frame grabber and their intensity $I_n(x, y)$ can be described as follows:

$$I_n(x, y) = R_n(x, y)\Big[A(x, y) + B(x, y)\cos(\varphi_n(x, y))\Big], \quad n = 1, 2, 3, ..., N \qquad (1)$$

where $R_n(x, y)$ is the object's surface reflectivity, $A(x, y)$ is the ambient light, $B(x, y)/A(x, y)$ is the fringe contrast, $\varphi_n(x, y)$ is the phase of the deformed fringe patterns modulated by the height of the object.

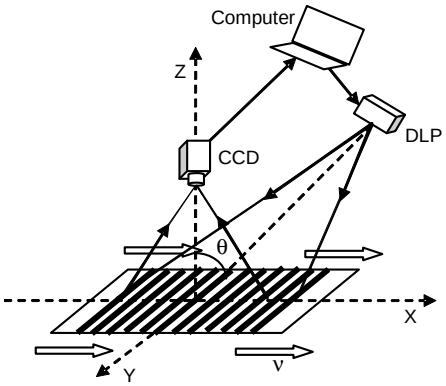

Fig. 1. On-line 3-D inspection system.

The motion of the inspected object before CCD results in the change of positions of the images in different deformed patterns, so the distributions of $R_n(x, y)$ and $\varphi_n(x, y)$ in different deformed patterns are different. The subscript n is used to distinguish them. In order to calculate the phase, pixel matching [14] must be carried out to guarantee that the images of the object in different deformed patterns have the same pixel position. The pixel matching also converts Δx (the motion of the object in equal time interval) to the equivalent phase-shifting step. A sequence of equivalent phase-shifting patterns are cut from the original deformed patterns after pixel matching, and their intensity can be described as follows:

$$I'_n(x, y) = R(x, y)\left\{A(x, y) + B(x, y)\cos\left[\varphi(x, y) + (n-1)\varphi_0\right]\right\}, \quad n = 1, 2, 3, ..., N \tag{2}$$

where φ_0 is the equivalent phase-shifting step. $R(x, y)$ is the object's surface reflectivity and $\varphi(x, y)$ is the phase of the deformed fringe patterns modulated by the height of inspected object. The pixel coordinate values of the object's image in different deformed patterns are uniform because they are adjusted by the process of pixel matching. So, the subscript n in $R_n(x, y)$ and $\varphi_n(x, y)$ in Eq. (1) can be omitted in Eq. (2).

Here, a reasonable choice of improved five-step Stoilov's algorithm [15, 16] makes the inspection more convenient to operate. Stoilov's algorithm is also an equal step length phase-shifting algorithm, but the value of phase-shifting is arbitrary; in other words, the sum of phase-shifting steps does not need to be integer multiple of 2π, which greatly reduces the requirement of control accuracy of measuring instrument. In Stoilov's algorithm, the value of N is 5 and the phase distribution can be calculated as follows:

$$\varphi(x, y) = \operatorname{atan}\left\{\frac{2\left[I'_2(x, y) - I'_4(x, y)\right]}{2I'_3(x, y) - I'_1(x, y) - I'_5(x, y)}\sin(\varphi_0)\right\} \tag{3}$$

and the phase-shifting $\sin(\varphi_0)$ is:

$$\sin\left[\varphi_0(x, y)\right] = \sqrt{1 - \left\{\frac{I_1'(x, y) - I_5'(x, y)}{2\left[I_2'(x, y) - I_4'(x, y)\right]}\right\}^2} \tag{4}$$

From Eq. (3), the values of the phase $\varphi(x, y)$ range from $-\pi$ to π and is discontinuous by an arctangent function. A phase-unwrapping algorithm is used to convert the sawtooth-like phase-wrapped image into a continuous phase distribution $\Psi(x, y)$. The height distribution $h(x, y)$ is restored by mapping the unwrapped phase $\Psi(x, y)$ into the height [17, 18]:

$$\frac{1}{h(x, y)} = a(x, y) + b(x, y)\frac{1}{\Psi(x, y)} + c(x, y)\frac{1}{\Psi^2(x, y)} \tag{5}$$

where $a(x, y)$, $b(x, y)$ and $c(x, y)$ depend on the parameter of system setup and require to be calibrated.

3. Pixel matching based on modulation

According to the process described above, pixel matching is a key procedure, which directly affects the measurement result of 3D on-line inspection. The process of pixel matching is described in the following subsections.

3.1. Extraction of modulation

Equation (1) is Fourier transformed and the Fourier spectrum is described as follows:

$$G_n(f_x, f_y) = P_n(f_x, f_y) + Q_n(f_x - f_1, f_y) + Q_n(f_x + f_1, f_y), \quad n = 1, 2, 3, ..., N \tag{6}$$

where $G_n(f_x, f_y)$, $P_n(f_x, f_y)$, $Q_n(f_x, f_y)$ represent the Fourier spectrum of $I(x, y)$, $R_n(x, y)A(x, y)$ and $R_n(x, y)B(x, y)$, respectively. A suitable band-pass filter is used to filter only the +1 order term of the Fourier spectrum and then inverse Fourier transform is carried out to deal with $Q_n(f_x - f_1, f_y)$:

$$g_n(x, y) = \int_{-\infty}^{\infty}\int Q_n(f_x - f_1, f_y)\exp\left[i2\pi(f_x x + f_y y)\right]\mathrm{d}f_x\mathrm{d}f_y = \frac{1}{2}R_n(x, y)B(x, y)\exp(i\varphi_n) \tag{7}$$

The distributions of modulation $M_n(x, y)$ are defined as the model of $g_n(x, y)$:

$$M_n(x, y) = \mathrm{abs}\left[g_n(x, y)\right] = \frac{1}{2}R_n(x, y)B(x, y), \quad n = 1, 2, 3, ..., N \tag{8}$$

Here, the modulation information of deformed fringe patterns includes reflectivity distribution $R_n(x, y)$ and grating contrast distribution $B(x, y)$. $B(x, y)$ can be regarded as a constant if the projected grating is of good uniformity. The reflectivity of object and reference plane are different, so the modulation can be used to distinguish the measured object from the reference plane. When the object is moving before the CCD, the images of the object in the deformed patterns change and cannot be distinguished from the fringes. Therefore, the modulation can act as a template to mark the change of the object positions.

3.2. Pixel matching

According to the contour of the object, a particular region C is cut from the first modulation pattern $M_1(x, y)$ in Eq. (8), which is used as a template. The regions with maximum degree of correlation are evaluated through the correlation calculation between the template and all the modulation patterns; the difference of the coordinate values of regions reflects the motion of the object. Here, the bidirectional greatest correlative coefficient matching law is used to calculate the relative displacement between all the deformed patterns [19].

The function of correlation is as follows [19]:

$$\mathrm{RL} = \frac{\sum_{j=1}^{J}\sum_{k=1}^{K} E_1(j,k)\,E_n(j,k)}{\left[\sum_{j=1}^{J}\sum_{k=1}^{K} E_1^2(j,k)\right]\times\left[\sum_{j=1}^{J}\sum_{k=1}^{K} E_n^2(j,k)\right]} \tag{9}$$

where $E_1(j, k)$ denotes the template C, $E_n(j, k)$ denotes a part of the n-th modulation $M_n(x, y)$ and keeps the same size as template C, j is the abscissa and k is the ordinate, J and K describe the size of the template.

According to the coordinate values of the regions with maximum degree of correlation in each modulation pattern $M_n(x, y)$, a sequence of equivalent phase--shifting fringe patterns $I_n'(x, y)$ with the same size are cut down from the original deformed patterns $I_n(x, y)$, and the pixel coordinates of measured object's image in $I_n'(x, y)$ are identical with each other. This process is regarded as pixel matching. In this way, the movement of object is translated to the grating's phase shifting, and Stoilov's algorithm is used to calculate the phase distribution handily.

4. Numerical simulation and experiment

4.1. Numerical simulation

To demonstrate the feasibility of the methods proposed, a numerical simulation is performed. As shown in Fig. 2, a "cone like" object is used as the moving object with a size of 402×417 pixels. Figure 3 shows the pixel matching process diagram. Figure 3**a** shows five simulative deformed patterns $I_n(x, y)$, the object is covered by

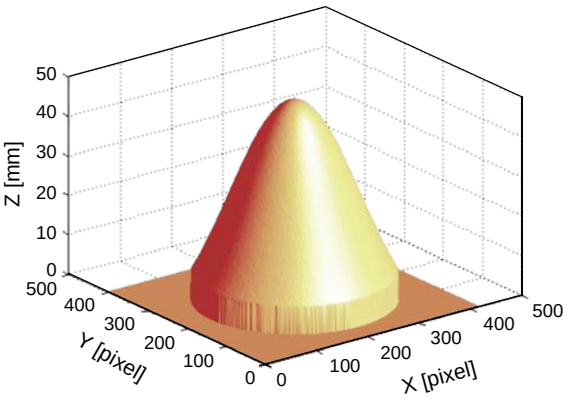

Fig. 2. Inspected object.

the fringes. Because of the movement of the object, the pixel coordinates of the images of measured object at each deformed pattern change. Figure 3**b** shows the corresponding modulation distributions. Figure 3**c** is a template cut from $M_1(x, y)$. It can be seen that the template is unique and can reflect the character of the measured object. Figure 3**d** shows the equivalent phase-shifting fringe patterns $I'_n(x, y)$ with the same pixel coordinate of the images, which are cut from Fig. 3**a** after pixel matching. Figure 4**a** is the 3-D reconstruction result. Figure 4**b** is the corresponding error distribution and its root mean square (RMS) value is 0.0149 mm.

4.2. Experiment

In order to verify the effectivity of the proposed method used in on-line 3-D inspection, a series of experiments were carried out. The experimental system is shown in Fig. 5. A sinusoidal fringe pattern is generated by a PC and projected onto the plane (used as a flowing-water production line where measured objects lie) by a DLP (CP-HX6500). The plane moves with a uniform speed, which is controlled by a step--motor (SC300-1A). CCD (MTV1881EX) which is controlled by a trigger signal captures the deformed fringe patterns with a constant frame rate and sends them to the PC to process.

One of the experiments is to inspect a “Mickey” moves with the work plane which is controlled by a step-motor. Figure 6**a** shows the inspected object; Fig. 6**b** shows one of the deformed patterns, Fig. 6**c** denotes the corresponding modulation. After pixel matching based on modulations, a sequence of equivalent phase-shifting fringe patterns with the same pixel coordinates of the images of measured object are obtained, and the calculation of wrapped phase is performed. Through unwrapping the wrapped phase and calculating the height from the unwrapped phase, the height reconstruction of object is completed according to Eq. (5), in which the parameters of the measurement setup [20, 21], $a(x, y)$, $b(x, y)$, and $c(x, y)$ are evaluated using a series of calibration planes. The reconstructed height distribution is shown in Fig. 6**d**. Because the actual height of the “Mickey” is unknown, the error analysis is not carried out. Under the same measurement setup, the traditional static PMP which is considered as

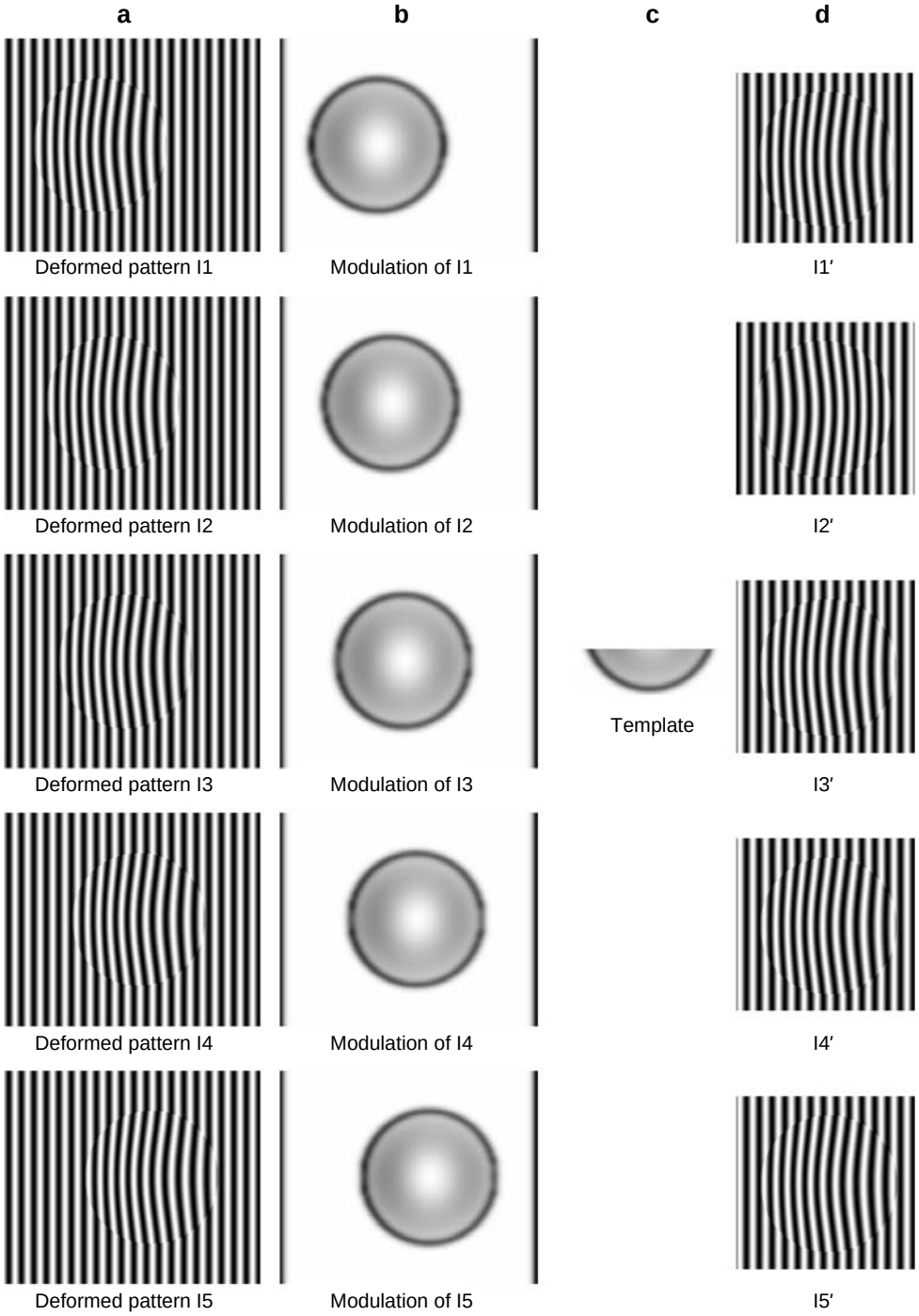

Fig. 3. Process of pixel matching: deformed patterns (**a**), modulations (**b**), template (**c**), and equivalent phase-shifting fringe patterns after pixel matching (**d**).

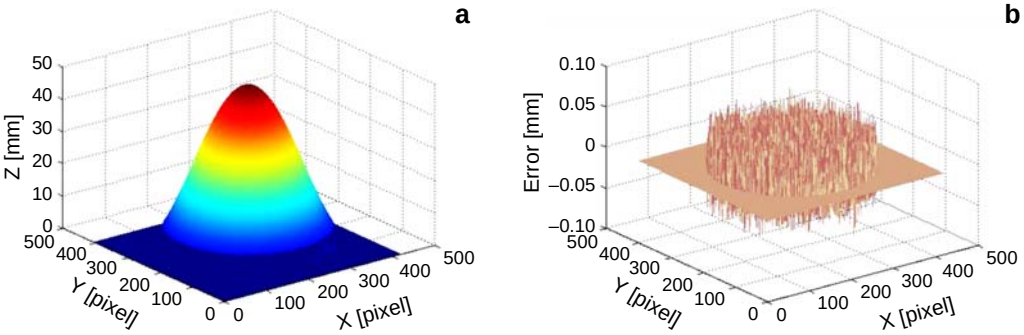

Fig. 4. Inspection result: 3-D reconstruction result (**a**) and error distribution (**b**).

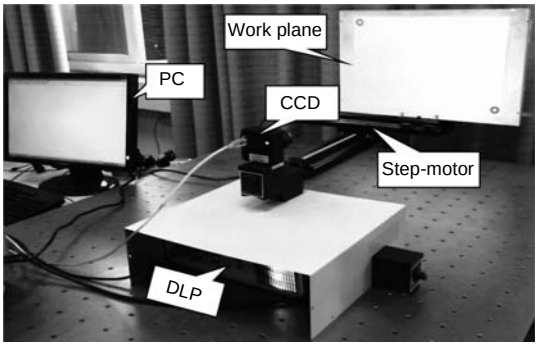

Fig. 5. The experimental system.

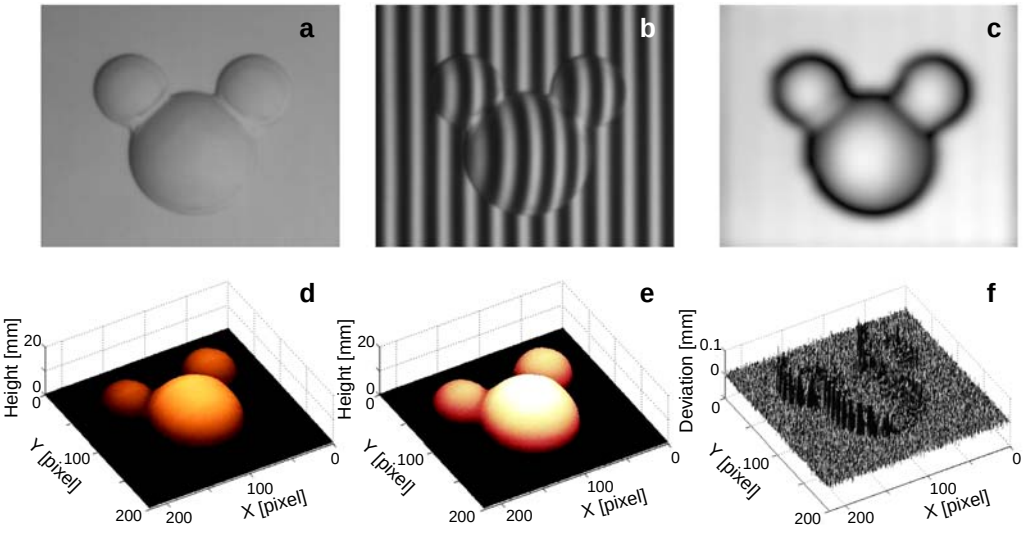

Fig. 6. Demonstration of accuracy: inspected object (**a**), deformed pattern (**b**), modulation (**c**), reconstruction result of the proposed method (**d**), reconstruction result of traditional static PMP (**e**) and deviation distribution (**f**).

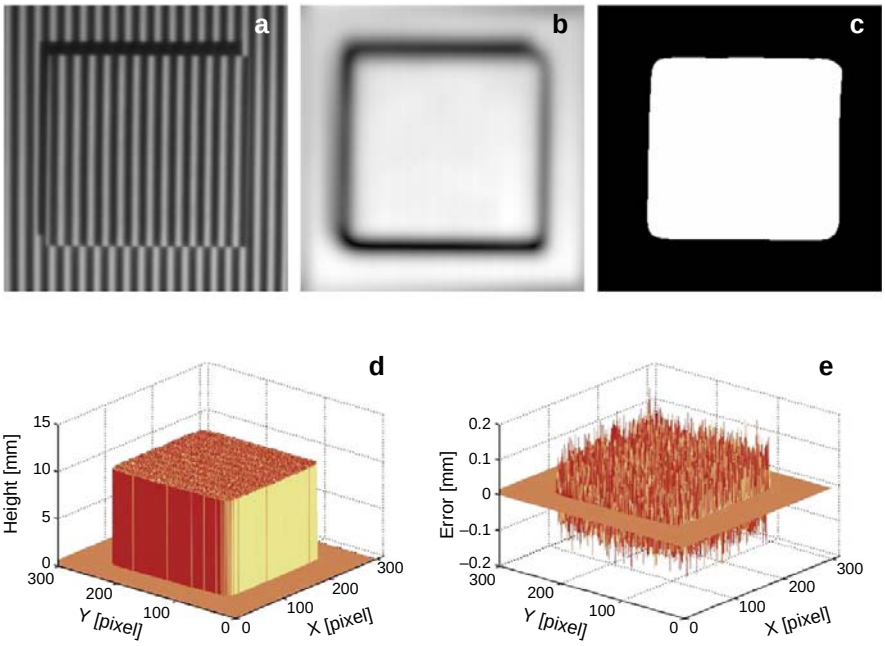

Fig. 7. Measurement of a gage plane: deformed pattern (**a**), modulation (**b**), mask (**c**), 3-D reconstruction of height (**d**) and error distribution (**e**).

a universal measurement method with high accuracy is used to restore the surface shape of the "Mickey". The restored result is shown in Fig. 6**e**. Figure 6**f** is the deviation distribution between the two reconstruction results. Its RMS value is 0.0233 and peak-to-valley (PV) value is 0.2602. It shows that the proposed on-line inspection method can restore the shape of object as the traditional static PMP and the deviation between the two measurement results is small. So, the proposed method has an approximate accuracy compared with the traditional static PMP.

In addition, to analyse the accuracy of the proposed approach, a gage plane with the height of 10 mm is measured using the above method. One of the deformed patterns is shown in Fig. 7**a**, and its corresponding modulation is shown in Fig. 7**b**. From Fig. 7**a**, we can see that the fringe is discontinuous at the edge of the plane due to the shadow. Therefore, we calculate the phase of the measured plane by using a "mask" to filter the shadow, and the "mask" is obtained through setting a threshold of modulation and is shown in Fig. 7**c**. The reconstruction height distribution of the tested plane is shown in Fig. 7**d**. The error distribution is shown in Fig. 7**e** and the RMS value is 0.0601 mm. It shows that the accuracy of the proposed method is considerable.

5. Conclusions

A novel on-line 3-D inspection method with PMP based on Stoilov's algorithm is proposed in this paper, which extends the application scope of the traditional PMP to

inspect the moving objects. In on-line 3-D inspection, the movement of inspected object leads to the displacement of images in deformed patterns, so pixel matching is required to obtain the equivalent phase-shifting which satisfies Stoilov's algorithm. Because modulation represents the contour of inspected object, modulation of the deformed pattern is originally used as a mark to implement the pixel matching in this paper. A region cut from the first modulation pattern acts as a template to implement correlation calculation with all the modulation patterns, and the regions with maximum degree of correlation in different modulation patterns are found. The difference of the positions of these regions which reflects the motion of object is converted to the equivalent phase-shifting, and the phase distribution is calculated with the equivalent phase-shifting patterns based on Stoilov's algorithm. Both numerical simulation and experiment verify the effectiveness and practicability of the proposed method.

References

[1] CHEN F., BROWN G.M., MUMIN SONG, *Overview of three-demensional shape measurement using optical methods*, Optical Engineering **39**(1), 2000, pp. 10–22.

[2] LURONG GUO, XIANYU SU, JIAN LI, *Improved Fourier transform profilometry for the automatic measurement of 3D object shapes*, Optical Engineering **29**(12), 1990, pp. 1439–1444.

[3] TAKEDA M., HIDEKI I., KOBOYASHI S., *Fourier-transform method of fringe-pattern analysis for computer-based topography and interferometry*, Journal of the Optical Society of America **72**(1), 1982, pp. 156–160.

[4] CHUNCAI WU, XIANYU SU, *Dynamic 3-D shape detected*, Optronics Laser **7**(5), 1996, pp. 273–278, (in Chinese)

[5] XIANYU SU, WHENJING CHEN, QICAN ZHANG, YIPING CAO, *Dynamic3-D shape measurement method based on FTP*, Optics and Lasers in Engineering **36**(1), 2001, pp. 49–64.

[6] LI ZHANG, CURLESS B., SEITZ S.M., *Rapid shape acquisition using color structured light and multi-pass dynamic programming*, Proceedings of the First International Symposium on 3D Data Processing Visualization and Transmission, 2002, pp. 24–36.

[7] SONG ZHANG, PEISEN S. HUANG, *High-resolution, real-time three-dimensional shape measurement*, Optical Engineering **45**(12), 2006, article 123601.

[8] SONG ZHANG, *Recent progresses on real-time 3D shape measurement using digital fringe projection techniques*, Optics and Lasers in Engineering **48**(2), 2010, pp. 149–158.

[9] LIKUN SU, XIANYU SU, WANGSONG LI, LIQUN XIANG, *Application of mudulation measurement profilometry to objects with surface holes*, Applied Optics **38**(7), 1999, pp. 1153–1158.

[10] JIAHUI PAN, PEISEN S. HUANG, FU-PEN CHIANG, *Color phase-shifting technique for three-dimensional shape measurement*, Optical Engineering **45**(1), 2006, article 013602.

[11] BERRYMAN F., PYNSENT P., CUBILLO J., *A theoretical comparison of three fringe analysis methods for determining the three-dimensional shape of an object in the presence of noise*, Optics and Lasers in Engineering **39**(1), 2003, pp. 35–50

[12] FARRELL C.T., PLAYER M.A., *Phase step mesaurement and variable step algorithms in phase-shifting interferometry*, Measurement Science and Technology **3**(10), 1992, pp. 953–958.

[13] YONEYAMA S., MORIMOTO Y., FUJIGAKI M., YABE M., *Phase-measuring profilometry of moving object without phase-shifting device*, Optics and Lasers in Engineering **40**(3), 2003, pp. 153–161.

[14] KO-CHEUNG HUI, WAN-CHI SIU, YUI-LAM CHAN, *New adaptive partial distortion search using clustered pixel matching error characteristic*, IEEE Transactions on Image Processing **14**(5), 2005, pp. 597–607

[15] STOILOV G., DRAGOSTINOV T., *Phase-stepping interferometry: Five-frame algorithm with an arbitrary step*, Optics and Lasers in Engineering **28**(1), 1997, pp. 61–69.
[16] XINFEN XU, YIPING CAO, *An improved Stoilov algorithm based on statistical approach*, Acta Sinica Sinica **29**(3), 2009, pp. 733–737, (in Chinese).
[17] WENSHEN ZHOU, XIANYU SU, *A direct mapping algorithm for phase-measurement profilometry*, Journal of Modern Optics **41**(1), 1994, pp. 89–94.
[18] WANSONG LI, XIANYU SU, ZHOUBAO LIU, *Large-scale three-dimensional object measurement: A practical coordinate mapping and image data-patching method*, Applied Optics **40**(20), 2001, pp. 3326–3333.
[19] JIANNING WU, BAOLONG GUO, ZONGZHE FENG, *An image mosaic technique based on interest points feature matching*, Journal of Optoelectronics, Laser **17**(6), 2006, pp. 733–737, (in Chinese).
[20] TAVARES P.J., VAZ M.A., *Linear calibration procedure for the phase-to-height relationship in phase measurement profilometry*, Optics Communications **274**(2), 2007, pp. 307–314.
[21] LEGARDA-SÁENZ R., BOTHE T., JÜPTNER W.P., *Accurate procedure for the calibration of a structured light system*, Optical Engineering **43**(2), 2004, pp. 464–471.

Received May 29, 2011
in revised form October 7, 2011